Joint Pilot and Phase Shift Design for IRS-assisted MIMO Communications

Gilderlan Tavares de Araújo and André L. F. de Almeida

Abstract— **Intelligent reflecting surface (IRS) is envisioned for beyond 5G systems due to its capacity to boost the spectral and energy efficiencies of wireless communications. The decoupled estimation of the involved communication channels is a non-trivial task in IRS-assisted wireless communications, especially for passive IRS structures. In this context, the joint design of the pilot sequences and the IRS phase shifts for channel estimation (CE) is challenging. In this paper, we provide an analytical solution to jointly design an optimal pilot and IRS phase shift matrices, leading to an improved CE performance. The solution consists of a factorization procedure that exploits the intrinsic Khatri-Rao structure of the combined pilot and phase shift matrices. This design is also used to obtain decoupled estimates of the individual channel matrices. Our results also show the noise rejection gain obtained from the proposed CE scheme compared to the conventional LS method. The proposed joint design offers a more efficient computation in terms of FLOPs and results in a faster channel estimation process than that of the individual design approach.**

Keywords— **Intelligent reflecting surface, channel estimation, MIMO, Khatri-Rao factorization.**

I. Introduction

The concept of Intelligent Reflecting Surfaces (IRS) holds great promise for the advancement of wireless communication networks beyond 5G and 6G [1], [2]. Recently, there has been a growing interest in investigating the use of IRS-assisted communication in various aspects of wireless communication, such as physical layer security [3] and non-orthogonal multiple access [4]. Additionally, the potential of the IRS in the context of joint communication and sensing has been explored [5]. The IRS is capable of passively altering characteristics of the incident electromagnetic wave, such as amplitude and phase. This represents a paradigm shift in wireless communication, where the wireless environment between a transmitter and receiver can be optimized to be more conducive to wave propagation [6].

The potential gains provided by the IRS requires a proper and optimized IRS phase shift, as well as optimum precoders and combines. This optimization, in turn, depends on the channel estimation accuracy, in general. As a result, channel estimation is crucial for the performance of the IRS-assisted system. Solutions to the CE problem have been presented in the literature, which range from conventional least squares (LS) methods to tensor modeling approaches (see [7] and references therein). The largest number of these solutions are pilot-assisted schemes. However, some semi-blind methods have been proposed to improve the spectral efficiency [8]–[10].

Solution to optimization problem has been presented in the literature for different scenarios, for example, MISO systems [11] where only the cascade channel (BS-IRS-Users) information is necessary and MIMO system [12] where the individual channel information (BS-IRS and IRS-User) are required. In this context, many works have been focused on the joint precoder and phase shifts design, while few works are dedicated to investigating the joint pilot and phase shift design [13], [14]. In this sense, the authors in [15] highlight the difficulty of a joint model/design for the IRS phase shift matrix and pilot symbols, while pointing out the challenge involved with a decoupled estimation of the individual communication channels. However, [10] decouples the individual channel by exploiting the Khatri-Rao structure of the cascaded channel. Still [9] proposes to decouple the channel beside the data symbol matrix in a semi-blind channel estimation method based on a tensor approach where a PARATUCK2 model was used. We can note that the optimization solutions resort to a numerical optimization problem in which a non-analytic solution is proposed where the knowledge of the channel covariance matrix is required.

Although the Khatri-Rao structure is present in IRS literature, as mentioned, to the best of your knowledge, there has been no investigation and evaluation of the denoising gain provided by the Khatri-Rao factorization in the IRS-assisted channel estimation approach. In the same way, as far as we know, the problem of jointly designing the pilot symbols and the IRS phase shifts analytically, i.e., without channel knowledge, has not yet been addressed in the literature. Since our proposed joint pilot and phase shift design does not requires channel knowledge, the choice of such parameters can be done offline avoiding using a dedicated time resource to define the optimal phase shifts in the LS sense and the pilot design. This means that, the CE, IRS, and pilot optimizations are considered independent problems. This paper has the following contributions:

- We exploit the intrinsic Khatri-Rao structure between the individual channel and show the denoising gains obtained by exploiting that Khatri-Rao structure.
- We show that the pilot matrix and the phase shifts matrix are linked by a Khatri-Rao product. Capitalizing on such a structure, we propose an analytical joint design for the

Gilderlan T. de Araújo is with Federal Institute of Ceará, Canindé, CE, e-mail: gilderlan.tavares@ifce.edu.br

André L. F. de Almeida is with Wireless Telecommunication Research Group (GTEL), Department of Teleinformatics, Federal University of Ceará, Fortaleza, CE, e-mail: andre@gtel.ufc.br.

This work was partially supported by the Ericsson Research, Sweden, and Ericsson Innovation Center, Brazil, under UFC.51 Technical Cooperation Contract Ericsson/UFC, and partially supported by Fundação Cearense de Apoio ao Desenvolvimento Científico e Tecnológico (FUNCAP) - Grant FC3-00198-00056.01.00/22. André L. F. de Almeida acknowledges CNPq for its financial support under the grant 312491/2020-4.

pilot and IRS phase shift matrices, leading to an optimal channel estimation method in the least squares sense.

To this end, we use a simple Khatri-Rao factorization to determine the optimal pilot and phase shifts matrices, which follow the orthogonality roles that are desired for an optimal design as can be seen in [13], and to show the CE denoising gain, as compared to the standard LS method, using a normalizes means square error as the performance metric. Further, using the Cramér–Rao bound (CRB) as a reference, we show that the proposed optimal design leads to theoretically optimal performance while improving the complexity in terms of the number of operations and runtime.

Notation and properties: Matrices are represented with boldface capital letters $\mathbf{A}$, and vectors are denoted by boldface lowercase letters $\mathbf{a}$. Transpose of a matrix $\mathbf{A}$ are denoted as $\mathbf{A}^{\mathrm{T}}$. The operator diag$(\mathbf{a})$ forms a diagonal matrix out of its vector argument, while $*$, $\diamond$, $\otimes$ denote the conjugate, Khatri Rao, and Kronecker products, respectively. $\mathbf{I}_N$ denotes the $N \times N$ identity matrix. The operator vec$(\cdot)$ vectorizes an $I \times J$ matrix argument, while unvec$_{I\times J}(\cdot)$ does the opposite operation. Besides, vecd$(\mathbf{A})$ forms a vector out its diagonal if $\mathbf{A}$ is a diagonal matrix. Moreover, $\mathbf{A}_{i.}$ denotes the ith row of the matrix $\mathbf{A}$. In this paper, we use the following properties:

$$(\mathbf{A} \otimes \mathbf{B})(\mathbf{C} \otimes \mathbf{D}) = \mathbf{AC} \otimes \mathbf{BD} \tag{1}$$

$$\mathrm{vec}(\mathbf{ABC}) = \left(\mathbf{C}^{\mathrm{T}} \otimes \mathbf{A}\right) \mathrm{vec}(\mathbf{B}), \text{ or} \tag{2}$$

$$\mathrm{vec}(\mathbf{ABC}) = \left(\mathbf{C}^{\mathrm{T}} \diamond \mathbf{A}\right) \mathrm{vecd}(\mathbf{B}) \tag{3}$$

if $\mathbf{B}$ is a diagonal matrix.

II. System Model

Let us consider an IRS-assisted Multiuser MIMO communication system with an unstructured channel model, for example in the sub 6-GHz band, where each user equipment (UE) is equipped with M_u antennas, the BS with L antennas, and the IRS has N passive reflecting elements. We assume that the direct (BS-UE) link is not available. In order to estimate the involved communication channels (UE-IRS and IRS-BS), pilot sequences are sent by the UE and the IRS reflects these pilots toward to BS using predetermined reflection patterns modeled as phase shifts. Then considering that the phase shifts vary at the pilot symbol rate the received signal at the BS can be written as

$$\begin{aligned}\mathbf{y}_{u,t} &= \mathbf{G}\mathrm{diag}(\boldsymbol{\phi}[t]) \sum_{u=1}^{U} \mathbf{H}_u^{\mathrm{T}} \mathbf{x}_u[t] \\ &= \mathbf{G}\mathrm{diag}(\boldsymbol{\phi}[t]) \left[\mathbf{H}_1^{\mathrm{T}} \ \ldots \ \mathbf{H}_U^{\mathrm{T}}\right] \begin{bmatrix} \mathbf{x}_1[t] \\ \vdots \\ \mathbf{x}_U[t] \end{bmatrix},\end{aligned} \tag{4}$$

where $\boldsymbol{\phi}[t] = \left[a_1 e^{j\beta_1[t]}, \, a_2 e^{j\beta_2[t]}, \, \ldots, \, a_N e^{j\beta_N[t]}\right]^{\mathrm{T}} \in \mathbb{C}^{N\times 1}$, denotes the phase shift vector, in which $\phi_n = a_n e^{j\beta_n[t]}$ where a_n and β_n denotes the amplitude and phase response from the n-th IRS element, $\mathbf{H}_u^{\mathrm{T}} \in \mathbb{C}^{N\times M_u}$ and $\mathbf{x}_u[t] \in \mathbb{C}^{M_u \times 1}$ correspond, respectively, to the channel between the IRS and the u-th user, and the pilot sequence transmitted by the u-th user. $\mathbf{G} \in \mathbf{C}^{L\times N}$ is the IRS-BS channel. M_u denotes the number of antennas associated with the u-th user. Note that this received signal described in equation (4), can be rewritten as

$$\mathbf{y}_t = \mathbf{G}\mathrm{diag}(\boldsymbol{\phi}[t])\mathbf{H}^{\mathrm{T}}\mathbf{x}[t] \,, \tag{5}$$

where $\mathbf{H}^{\mathrm{T}} = \left[\mathbf{H}_1^{\mathrm{T}} \ldots \mathbf{H}_K^{\mathrm{T}}\right] \in \mathbb{C}^{N\times M}$, and $\mathbf{x}[t] = [\mathbf{x}_1[t] \ldots \mathbf{x}_K[t]] \in \mathbb{C}^{M\times T}$ is the vector that collect all pilot sequences transmitted from all users, with $M = \sum_{k=1}^{K} M_k$. By applying the vec$(\cdot)$ operator in (5), we obtain

$$\begin{aligned}\mathbf{y}[t] &= \mathrm{vec}\left(\mathbf{G}\mathrm{diag}(\boldsymbol{\phi}[t])\mathbf{H}^{\mathrm{T}}\mathbf{x}[t]\right) \\ &= \left(\mathbf{x}[t]^{\mathrm{T}} \otimes \mathbf{I}_L\right)(\mathbf{H} \diamond \mathbf{G})\,\boldsymbol{\phi}[t]. \text{ (c.f. (3))}\end{aligned} \tag{6}$$

Applying once more the vec$(\cdot)$ operator, we can rewrite (6) as

$$\mathbf{y}[t] = \left(\boldsymbol{\phi}[t]^{\mathrm{T}} \otimes \mathbf{x}[t]^{\mathrm{T}} \otimes \mathbf{I}_L\right) \mathrm{vec}(\mathbf{H} \diamond \mathbf{G}) \,. \tag{7}$$

Collecting the received signals $\mathbf{y}[1], \ldots, \mathbf{y}[T]$ during the T symbol periods, we get:

$$\mathbf{y} = \begin{bmatrix} \mathbf{y}[1] \\ \vdots \\ \mathbf{y}[T] \end{bmatrix} = \left(\begin{bmatrix} \boldsymbol{\phi}[1]^{\mathrm{T}} \otimes \mathbf{x}[1]^{\mathrm{T}} \\ \vdots \\ \boldsymbol{\phi}[T]^{\mathrm{T}} \otimes \mathbf{x}[T]^{\mathrm{T}} \end{bmatrix} \otimes \mathbf{I}_L \right) \mathrm{vec}(\mathbf{H} \diamond \mathbf{G}) \,, \tag{8}$$

or, more compactly,

$$\begin{aligned}\mathbf{y} &= \left([\boldsymbol{\Phi} \diamond \mathbf{X}]^{\mathrm{T}} \otimes \mathbf{I}_L\right) \mathrm{vec}(\mathbf{H} \diamond \mathbf{G}) \\ &= \left(\mathbf{U}^{\mathrm{T}} \otimes \mathbf{I}_L\right) \boldsymbol{\theta} = \mathbf{W}\boldsymbol{\theta},\end{aligned} \tag{9}$$

where $\boldsymbol{\Phi} = \left[\boldsymbol{\phi}[1], \ldots, \boldsymbol{\phi}[T]\right] \in \mathbb{C}^{N\times T}$ and $\mathbf{X} = \left[\mathbf{x}[1], \ldots, \mathbf{x}[T]\right] \in \mathbb{C}^{M\times T}$ collect the phase shifts and pilot symbols during the T symbol periods, respectively, while $\mathbf{U} = \boldsymbol{\Phi} \diamond \mathbf{X} \in \mathbb{C}^{MN\times T}$, $\mathbf{W} = \left(\mathbf{U}^{\mathrm{T}} \otimes \mathbf{I}_L\right) \in \mathbb{C}^{TL\times MNL}$, and $\boldsymbol{\theta} = \mathrm{vec}(\mathbf{H} \diamond \mathbf{G}) \in \mathbb{C}^{MNL\times 1}$. The extension to include the direct link, if available, is straightforward.[1]

Note that the received signal model described in (9) has in-fact two Khatri-Rao structured matrices. The first one involves the "equivalent" MIMO channel combining $\mathbf{G}$ and $\mathbf{H}$, whose vectorized form is represented by $\boldsymbol{\theta}$. Such a Khatri-Rao structure was exploited in [16] to devise a closed-form channel estimation method. The second Khatri-Rao structured matrix is $\mathbf{U}$, which combines the IRS phase shift matrix and the pilot symbol matrix. In the related literature, the IRS phase shifts ($\boldsymbol{\Phi}$) and pilot symbols ($\mathbf{X}$) are designed separately [17], [18]. Here, by exploiting the Khatri-Rao structure of $\mathbf{U}$, *we propose a joint design of* $\boldsymbol{\Phi}$ *and* $\mathbf{X}$ *from an exact Khatri-Rao factorization of* $\mathbf{U}$. Note that such a structure naturally appears when modeling channel estimation problems.

III. Joint Phase Shift and Pilot Design

The LS estimate to (9) is given by

$$\hat{\boldsymbol{\theta}} = \arg\min_{\boldsymbol{\theta}} |\mathbf{W}\boldsymbol{\theta} - \mathbf{y}|_2^2, \tag{10}$$

the solution of which is found as

$$\hat{\boldsymbol{\theta}} = \left(\mathbf{W}^{\mathrm{H}}\mathbf{W}\right)^{-1} \mathbf{W}^{\mathrm{H}}\mathbf{y}. \tag{11}$$

[1] If the direct link is available, the received signal in (9) is written as $\mathbf{y} = ([\widetilde{\boldsymbol{\Phi}} \diamond \mathbf{X}]^{\mathrm{T}} \otimes \mathbf{I}_L)\overline{\boldsymbol{\theta}}$ where $\widetilde{\boldsymbol{\Phi}} = [\boldsymbol{\Phi}^{\mathrm{T}} \quad \mathbf{1}_T^{\mathrm{T}}]^{\mathrm{T}} \in \mathbb{C}^{(N+1)\times T}$ and $\overline{\boldsymbol{\theta}} = [\mathrm{vec}(\mathbf{H} \diamond \mathbf{G})^{\mathrm{T}} \quad \mathrm{vec}(\mathbf{H}_{\mathrm{d}})^{\mathrm{T}}]^{\mathrm{T}} \in \mathbb{C}^{LM(N+1)\times 1}$, where $\mathbf{H}_{\mathrm{d}} \in \mathbb{C}^{L\times M}$ is the direct link MIMO channel matrix.

This estimator attains the Cramér Rao Bound (CRB) [19], and its optimal solution is achieved when $\mathbf{W}$ is an column-orthogonal semi-unitary matrix, which implies that

$$\begin{aligned}\mathbf{W}^{\mathrm{H}}\mathbf{W} &= (\mathbf{U}^{*}\otimes\mathbf{I}_L)\left(\mathbf{U}^{\mathrm{T}}\otimes\mathbf{I}_L\right)\\ &= (\mathbf{U}^{*}\mathbf{U}^{\mathrm{T}}\otimes\mathbf{I}_L) = T\mathbf{I}_{MNL}.\ \text{(c.f. (1))}\end{aligned} \tag{12}$$

This condition means that $\mathbf{U} = \mathbf{\Phi}\diamond\mathbf{X}$ should be a *row-orthogonal semi-unitary matrix*. A feasible choice that leads to an optimum performance consists of choosing $\mathbf{U}$ as the first MN rows of a $T\times T$ DFT matrix, where $T \geq MN$. Then, let $\mathbf{U}\in\mathbb{C}^{MN\times T}$ be constructed by truncating a DFT matrix to its first MN rows. Defining $\mathbf{u}_t\in\mathbb{C}^{MN\times 1}$ as the t-th column of $\mathbf{U}$. Since $\mathbf{u}_t$ is a Vandermonde vector, we have

$$\mathbf{u}_t = \begin{bmatrix} 1 \\ u^{Mt} \\ \vdots \\ u^{M(N-1)t}\end{bmatrix} \otimes \begin{bmatrix} 1 \\ u^{t} \\ \vdots \\ u^{(M-1)t}\end{bmatrix},\ t=1,\ldots,T. \tag{13}$$

Defining

$$\mathbf{\Phi}_{.t} \doteq \left[1, u^{Mt},\ldots,u^{M(N-1)t}\right]^{\mathrm{T}} \in\mathbb{C}^{N\times 1}, \tag{14}$$

and

$$\mathbf{X}_{.t} \doteq \left[1, u^{t},\ldots,u^{(M-1)t}\right]^{\mathrm{T}} \in\mathbb{C}^{M\times 1}, \tag{15}$$

it follows that

$$\mathbf{u}_t = \mathbf{\Phi}_{.\,t}\otimes\mathbf{X}_{.\,t},\quad t=1,\ldots,T, \tag{16}$$

which implies that

$$\mathbf{U} = [\mathbf{\Phi}_{.1}\otimes\mathbf{X}_{.1},\ldots,\mathbf{\Phi}_{.T}\otimes\mathbf{X}_{.T}] = \mathbf{\Phi}\diamond\mathbf{X}\in\mathbb{C}^{MN\times T}. \tag{17}$$

Hence, the pilot symbol matrix and the IRS phase shifts matrix have, respectively, the following structure

$$\mathbf{\Phi} = \begin{bmatrix} 1 & 1 & \cdots & 1 \\ 1 & u^{M} & \cdots & u^{M(T-1)} \\ \vdots & \vdots & \ddots & \vdots \\ 1 & u^{M(N-1)} & \cdots & u^{M(N-1)(T-1)}\end{bmatrix} \in\mathbb{C}^{N\times T}, \tag{18}$$

and

$$\mathbf{X} = \begin{bmatrix} 1 & 1 & \cdots & 1 \\ 1 & u & \cdots & u^{(T-1)} \\ \vdots & \vdots & \ddots & \vdots \\ 1 & u^{(M-1)} & \cdots & u^{(M-1)(T-1)}\end{bmatrix} \in\mathbb{C}^{M\times T}. \tag{19}$$

Note that, taken $\mathbf{U}$ as a $MN\times T$ DFT matrix, with $T\geq MN$, the pilot symbol matrix $\mathbf{X}$ corresponds to a truncation of its first M rows, while the IRS phase shift matrix corresponds to a selection of its N rows. Therefore, for fixed system parameters M, N, and T, our design extracts the pilot symbol matrix and the IRS phase shift matrix from an exact Khatri-Rao factorization of a single DFT codebook matrix, as shown in Eq. (17). Moreover, this design leads to an optimum LS channel estimation due to the semi-orthogonal structure of the $\mathbf{U}$, satisfying condition (12). A summary of the DFT factorization procedure to find the pilot symbol matrix and the IRS phase shifts from $\mathbf{U}$ is given in Algorithm 1.

Algorithm 1: DFT factorization

Procedure
input : A DFT matrix $\mathbf{U}\in\mathbb{C}^{T\times T}$
output: $\mathbf{\Phi}\in\mathbb{C}^{N\times T}$ and $\mathbf{X}\in\mathbb{C}^{M\times T}$
begin
  $\mathbf{X}\longleftarrow\mathbf{U}(1:M,:)$, $\mathbf{X}$ is a truncated DFT (t-DFT)
  for $n=1,\ldots,N$ **do**
    $\mathbf{\Phi}(n,:) = \mathbf{U}((n-1)M+1,:)$
End

Remark: The condition $T\geq MN$ can be not feasible, in particular when the number of IRS elements increases. As a solution for this problem different authors proposes an element grouping strategy [7] This strategy can reduce the IRS gains, however, optimization of the element grouping has been investigated [20].

IV. Noise rejection gain

Once the LS estimate of the channel parameter vector $\boldsymbol{\theta}$ is obtained from (10), decoupled estimates of the IRS-UEs and BS-IRS channels can be extracted by capitalizing on its intrinsic Khatri-Rao structure [16], since $\boldsymbol{\theta} = \mathrm{vec}(\mathbf{H}\diamond\mathbf{G})$. We now show that this process enhances the channel estimation procedure due to an additional noise rejection gain. To see this, let us define $\mathbf{\Omega} = \mathrm{unvec}_{ML\times N}(\hat{\boldsymbol{\theta}}) = \hat{\mathbf{H}}\diamond\hat{\mathbf{G}}\in\mathbb{C}^{ML\times N}$. Its n-th column can be factorized as $\boldsymbol{\omega}_n = \hat{\mathbf{h}}_n\otimes\hat{\mathbf{g}}_n$, which can be reshaped as $\mathbf{\Omega}_n = \mathrm{unvec}_{L\times M}(\boldsymbol{\omega}_n) = \hat{\mathbf{g}}_n\hat{\mathbf{h}}_n^{\mathrm{T}}\in\mathbb{C}^{L\times M}$. Since $\mathbf{\Omega}_n$ can be approximated as a rank one matrix, the best estimates of $\mathbf{g}_n$ and $\mathbf{h}_n$ can be found from the dominant left and right singular vectors of $\mathbf{\Omega}_n$, respectively, i.e. $\hat{\mathbf{h}}_n = \sqrt{\sigma_1}\mathbf{v}_1^{*}$ and $\hat{\mathbf{g}}_n = \sqrt{\sigma_1}\mathbf{u}_1$. A pseudocode can be found in [16]. Note that each rank one approximation applied to $\mathbf{\Omega}_n$ involves discarding $\min(M,L)-1$ singular values associated with its noise subspace. We can then compute a noise rejection measure associated with the estimation of $\mathbf{g}_n$ and $\mathbf{h}_n$ as

$$R_n = \sum_{r=2}^{\min(M,L)} \sigma_n(r),\quad n=1,\ldots,N, \tag{20}$$

where $\sigma_n(r)$ denotes the r-th singular value of the matrix $\mathbf{\Omega}_n$, $r=1,\ldots,\min(M,L)$. The noise rejection gain associated with the decoupled estimation of $\mathbf{G}$ and $\mathbf{H}$ is then given by

$$\mathrm{NR} = \sum_{n=1}^{N}\frac{R_n}{\|\mathbf{\Omega}_n\|_F}. \tag{21}$$

In summary, this equation provides the sum-ratio of the energy of the noise subspace and the energy of the whole space of the set of matrices $\mathbf{\Omega}_1,\ldots,\mathbf{\Omega}_N$, yielding a relative measure of how much estimation noise is rejected when the decoupled estimates of $\mathbf{G}$ and $\mathbf{H}$ are extracted from $\hat{\boldsymbol{\theta}}$ by leveraging its intrinsic Khatri-Rao structure.

V. Complexity analysis

We investigate in this section the impact of the proposed method in the CE and optimal as well as over the calculation of the optimal pilot and phase shifts matrices.

A. Complexity to obtain the channel estimation

The joint orthogonal design of the phase shift matrix and the pilot matrix is also beneficial from a computational viewpoint, since it results in a lower overall complexity of the LS solution (10). Note that under the orthogonality assumption for $\mathbf{U} = \mathbf{\Phi} \diamond \mathbf{X} \in \mathbb{C}^{MN \times T}$, the LS estimate in (10) simplifies to

$$\hat{\boldsymbol{\theta}} = \frac{1}{T}\mathbf{W}^{\mathrm{H}}\mathbf{y} = (\mathbf{U}^{*} \otimes \mathbf{I}_{L})\mathbf{y} = \mathrm{vec}(\mathbf{Y}\mathbf{U}^{\mathrm{H}}), \qquad (22)$$

where $\mathbf{Y} \doteq \mathrm{unvec}_{L \times T}(\mathbf{y}) \in \mathbb{C}^{L \times T}$. The complexity to estimate the cascaded channel from (22) using the proposed joint orthogonal design is $\mathcal{O}(LTMN)$. Channel decoupling via the Khatri Rao factorization (KRF) procedure requires N SVD steps, which leads to a complexity of $\mathcal{O}(MNL)$. Thus the total complexity of decoupling the channel using our proposed orthogonal design is $\mathcal{O}(MNL(T+1))$.

B. Complexity to determine the optimal joint pilot and phase shifts design

This process can be carried out offline, which means that the complexity to provide the optimal pilot and phase shift matrix design is zero since this procedure can be done before the start of the transmission process. Then, our proposed joint pilot and phase shift design is less complex than any other online method. To summarize, note that in our solution, the matrix $\mathbf{U}$ can be chosen from a DFT codebook and then using the algorithm 1 to design $\mathbf{X}$ and $\mathbf{\Phi}$.

VI. Cramér-Rao Bound

Let us recall the linear model given by equation (9) as

$$\mathbf{y} = \left(\mathbf{U}^{\mathrm{T}} \otimes \mathbf{I}_{L}\right)\boldsymbol{\theta} = \mathbf{W}\boldsymbol{\theta},$$

in which the solution $\hat{\boldsymbol{\theta}}$ is given by the MVU estimator (11) with covariance matrix $\mathrm{Cov}(\hat{\boldsymbol{\theta}}) = \sigma^{2}\left(\mathbf{W}^{\mathrm{H}}\mathbf{W}\right)^{-1}$, the design of the matrix $\mathbf{W}$ directly impacts the estimation variance. For attaining the minimum variance possible $\mathbf{W}^{\mathrm{H}}\mathbf{W}$ should be diagonal (see [21], p. 93). In our proposal $\mathbf{W}^{\mathrm{H}}\mathbf{W} = T\mathbf{I}_{MNL}$. Thus,

$$\mathrm{Cov}(\hat{\boldsymbol{\theta}})_{i,i} = \mathrm{var}(\hat{\boldsymbol{\theta}}_{i}) = \frac{\sigma^{2}MNL}{T}. \qquad (23)$$

For the proposed joint design of $\mathbf{\Phi}$ and $\mathbf{X}$, the condition (23) is satisfied always since that $\mathbf{U}$ is ensured to be row-orthogonal.

VII. Simulation Results

In this section, we present some numerical results to corroborate the advantage of the proposed joint design of phase shifts and pilot symbols. To this end, we evaluate the noise rejection gain (cf. equations (20) and (21)), the normalised mean square error (NMSE) of the estimated channels, defined as $\mathrm{NMSE} = \|\boldsymbol{\theta} - \hat{\boldsymbol{\theta}}\|_{F}^{2}/\|\boldsymbol{\theta}\|_{F}^{2}$, and the computational complexity of the KRF channel estimation method. We consider $N = 100$ and $L = M$, with $M = 2, 3 \ldots, 10$. The total training time is fixed to $T = 10N$ symbols to satisfy the condition $T \geq NM$. As a reference, we also depict the CRB for $M = L = 3$, $N = 20$, and consequently $T = 60$.

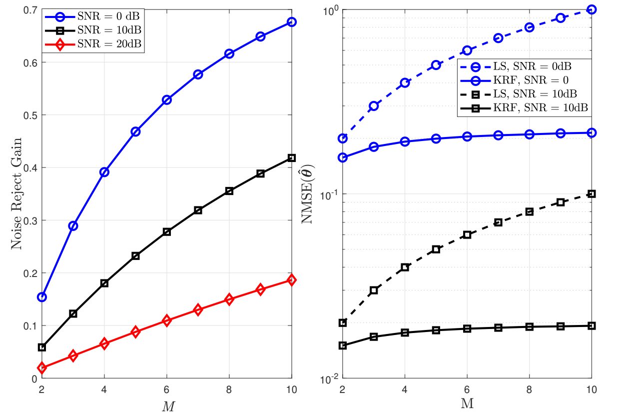

Fig. 1: Noise rejection gain.

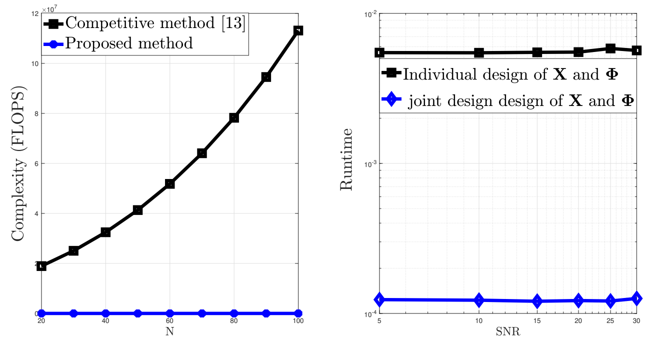

Fig. 2: Complexity analysis

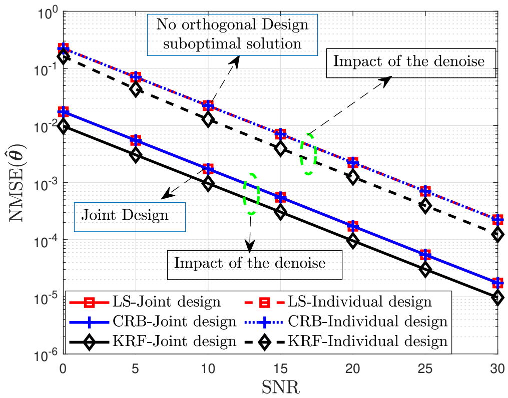

Fig. 3: Joint design vs. individual design, and the CRB.

Figure 1 shows the noise rejection gain associated with the estimation of the channel parameter vector $\boldsymbol{\theta} = \mathrm{vec}(\mathbf{H} \diamond \mathbf{G})$ for different SNR levels and numbers of transmit/receive antennas. Note that the noise rejection level increases as more transmit and/or receive antennas are used. Such a noise rejection gain translates into an enhanced estimation of the channel parameter vector in comparison with the LS channel estimator, thanks to the extraction of the individual estimates of $\mathbf{G}$ and $\mathbf{H}$ via the KRF algorithm (see Fig. 1 left side). Also, the NMSE performance of the LS estimator degrades as more antennas are used due to the higher number of channel parameters to be estimated. In contrast, the KRF estimator is much less sensitive to the increase of M and/or L, corroborating the noise rejection gain obtained by this method (see Fig. 1 left side). Recall that the LS estimator is limited to obtain the unstructured estimate of $\boldsymbol{\theta}$ according to (10), while the KRF estimator additionally exploits the Khatri-Rao structure present in $\boldsymbol{\theta}$ as shown in (9) to find decoupled estimates of $\mathbf{G}$ and $\mathbf{H}$, and then rebuilds the estimation of $\boldsymbol{\theta}$ from the individual ("cleaner") channel estimates.

In Figure 2, we compare the computational complexity with a reference method in terms of the operations associated with joint design procedure and CE. In particular, assuming $M = L = 10$, $T = 3000$, and $N \in \{10, 20, 30, \ldots, 100\}$, these results show that the proposed joint design of the pilot and phase shifts determines $\mathbf{X}$ and $\boldsymbol{\Phi}$ with less arithmetic operations in comparison with competitive method [13], which have a similar overhead and complexity $\mathcal{O}(N + L^2)^{3.5}$ (see Fig. 2 left side). Further, note that the matrix $\mathbf{U}$ in (22) is orthogonal, avoiding the computation of a matrix inverse. On the other hand, if $\mathbf{U}$ is obtained from the individual designs of $\boldsymbol{\Phi}$ and $\mathbf{X}$, such an orthogonality property cannot be ensured, even when $\mathbf{X}$ and $\boldsymbol{\Phi}$ individually meeting the conditions of orthogonality required to be considered an optimal design. In this sense, we show that design $\boldsymbol{\Phi}$ and $\mathbf{X}$ jointly, which ensure the orthogonality, becomes the CE around 44 times faster than the individual design, where the orthogonality of $\mathbf{U}$ is not ensured (see Fig. 1 right side).

Figure 3, we use a CRB as a benchmark to compare the performance when the individual designs of $\boldsymbol{\Phi}$ and $\mathbf{X}$ are considered. Thus, considering $\boldsymbol{\Phi}$ and $\mathbf{X}$ as truncated DFT and Hadamard matrices, respectively. We can note that the NMSE of the LS solution attains the CRB, which is expected since it is an minimum variance unbiased (MVU) estimator. However, we can observe a remarkable gain of the proposed joint design over the individual design approach, while the KRF procedure improves the channel estimation accuracy due to the denoising property.

VIII. Conclusions

A joint design for the phase shift and pilot matrices in an IRS-assisted multi-user MIMO system was proposed, which is based on an exact Khatri-Rao factorization of a DFT matrix, leading to an optimal estimate of the composite channel. The proposed joint design offers an improved NMSE performance while being less complex for determining jointly the pilot and phase shifts matrices in comparison with the competitor method, whereas become the CE is more efficient in terms of runtime in comparison with the individual design approach, where phase shifts and pilots are individually designed. In addition, exploiting the Khatri-Rao product structure of the composite channel provides a noise rejection gain, leading to more accurate estimates of the individual channels, compared with the standard LS estimator that ignores such a structure.

References

[1] Z. Zhang, L. Dai, X. Chen, C. Liu, F. Yang, R. Schober, and H. V. Poor, "Active RIS vs. passive RIS: Which will prevail in 6G?" *IEEE Trans. Commun.*, vol. 71, no. 3, pp. 1707–1725, 2023.

[2] Y. Huo, X. Lin, B. Di, H. Zhang, F. J. L. Hernando, A. S. Tan, S. Mumtaz, Ö. T. Demir, and K. Chen-Hu, "Technology trends for massive MIMO towards 6G," *arXiv preprint arXiv:2301.01703*, 2023.

[3] X. Lu, L. Xiao, P. Li, X. Ji, C. Xu, S. Yu, and W. Zhuang, "Reinforcement learning-based physical cross-layer security and privacy in 6G," *IEEE Commun. Surveys Tuts.*, vol. 25, no. 1, pp. 425–466, 2023.

[4] T. H. T. Le, L. Cantos, S. R. Pandey, H. Shin, and Y. H. Kim, "Federated learning with noma assisted by multiple intelligent reflecting surfaces: Latency minimizing optimization and auction," *IEEE Trans. Veh. Technol.*, pp. 1–16, 2023.

[5] X. Cao, X. Hu, and M. Peng, "Feedback-based beam training for intelligent reflecting surface aided mmwave integrated sensing and communication," *IEEE Trans. Veh. Technol.*, pp. 1–12, 2023.

[6] M. Di Renzo, A. Zappone, M. Debbah, M.-S. Alouini, C. Yuen, J. de Rosny, and S. Tretyakov, "Smart radio environments empowered by reconfigurable intelligent surfaces: How it works, state of research, and the road ahead," *IEEE J. Sel. Areas in Commun.*, vol. 38, no. 11, pp. 2450–2525, 2020.

[7] B. Zheng, C. You, W. Mei, and R. Zhang, "A survey on channel estimation and practical passive beamforming design for intelligent reflecting surface aided wireless communications," *IEEE Commun. Surveys Tuts.*, vol. 24, no. 2, pp. 1035–1071, 2022.

[8] L. Wei, C. Huang, Q. Guo, Z. Yang, Z. Zhang, G. C. Alexandropoulos, M. Debbah, and C. Yuen, "Joint channel estimation and signal recovery for RIS-empowered multiuser communications," *IEEE Trans. Commun.*, vol. 70, no. 7, pp. 4640–4655, Jul. 2022.

[9] G. T. de Araújo, A. L. F. de Almeida, R. Boyer, and G. Fodor, "Semi-blind joint channel and symbol estimation for IRS-assisted MIMO systems," *IEEE Trans. Signal Process.*, vol. 71, pp. 1184–1199, 2023.

[10] G. T. de Araújo, P. R. B. Gomes, A. L. F. de Almeida, G. Fodor, and B. Makki, "Semi-blind joint channel and symbol estimation in IRS-assisted multiuser MIMO networks," *IEEE Wireless Commun. Lett.*, vol. 11, no. 7, pp. 1553–1557, 2022.

[11] Z. Zhou, N. Ge, Z. Wang, and L. Hanzo, "Joint transmit precoding and reconfigurable intelligent surface phase adjustment: A decomposition-aided channel estimation approach," *IEEE Trans. Commun.*, vol. 69, no. 2, pp. 1228–1243, 2021.

[12] A. Zappone, M. Di Renzo, F. Shams, X. Qian, and M. Debbah, "Overhead-aware design of reconfigurable intelligent surfaces in smart radio environments," *IEEE Trans. Wireless Commun.*, vol. 20, no. 1, pp. 126–141, Jan. 2021.

[13] J.-M. Kang, "Intelligent reflecting surface: Joint optimal training sequence and refection pattern," *IEEE Commun. Lett.*, vol. 24, no. 8, pp. 1784–1788, Apr. 2020.

[14] Z. Sun, X. Wang, S. Feng, X. Guan, F. Shu, and J. Wang, "Pilot optimization and channel estimation for two-way relaying network aided by IRS with finite discrete phase shifters," *IEEE Trans. Veh. Technol.*, vol. 72, no. 4, pp. 5502–5507, 2023.

[15] N. T. Nguyen, J. He, V.-D. Nguyen, H. Wymeersch, D. W. K. Ng, R. Schober, S. Chatzinotas, and M. Juntti, "Hybrid relay-reflecting intelligent surface-aided wireless communications: Opportunities, challenges, and future perspectives," 2021, arXiv:2104.02039v2 [eess.SP].

[16] G. T. de Araújo, A. L. F. de Almeida, and R. Boyer, "Channel estimation for intelligent reflecting surface assisted MIMO systems: A tensor modeling approach," *IEEE J. Sel. Topics Signal Process.*, vol. 15, no. 3, pp. 789–802, Feb. 2021.

[17] T. Jiang, H. V. Cheng, and W. Yu, "Learning to beamform for intelligent reflecting surface with implicit channel estimate," in *proc. GLOBECOM "2020"*, pp. 1–6.

[18] J. Zhang, C. Qi, P. Li, and P. Lu, "Channel estimation for reconfigurable intelligent surface aided massive MIMO system," in *proc. SPAWC "2020"*, pp. 1–5.

[19] T. L. Jensen and E. De Carvalho, "An optimal channel estimation scheme for intelligent reflecting surfaces based on a minimum variance unbiased estimator," in *Proc. ICASSP "2020"*, pp. 5000–5004.

[20] N. K. Kundu, Z. Li, J. Rao, S. Shen, M. R. McKay, and R. Murch, "Optimal grouping strategy for reconfigurable intelligent surface assisted wireless communications," *IEEE Wireless Commun. Lett.*, vol. 11, no. 5, pp. 1082–1086, May 2022.

[21] S. M. Kay, *Fundamentals of Statistical Signal Processing: Estimation Theory*. Prentice Hall, 1997.